ELSEVIER

Contents lists available at ScienceDirect

# Journal of Membrane Science

journal homepage: http://www.elsevier.com/locate/memsci





# Freestanding self-assembled sulfonated pentablock terpolymer membranes for high flux pervaporation desalination

Elisabeth R. Thomas <sup>a,f,1</sup>, Amit Jain <sup>b,f,1</sup>, Stewart C. Mann <sup>a,f</sup>, Yi Yang <sup>a,f</sup>, Matthew D. Green <sup>a,f</sup>, W. Shane Walker <sup>e,f</sup>, François Perreault <sup>d,f</sup>, Mary Laura Lind <sup>a,f,\*</sup>, Rafael Verduzco <sup>b,c,f,\*\*</sup>

- <sup>a</sup> School for Engineering of Matter, Transport and Energy, Arizona State University, Tempe, AZ, 85287, USA
- <sup>b</sup> Department of Chemical and Biomolecular Engineering, Rice University, MS 362, 6100 Main Street, Houston, USA
- <sup>c</sup> Material Science and Nanoengineering, Rice University, MS 325, 6100 Main Street, Houston, USA
- d School of Sustainable Engineering and the Built Environment, Arizona State University, Tempe, AZ, 85287-3005, USA
- <sup>e</sup> Civil Engineering, The University of Texas at El Paso, 500 W University Avenue, El Paso, TX, 79912, USA
- f NSF Nanosystems Engineering Research Center Nanotechnology-Enabled Water Treatment, Rice University, MS 6398, 6100 Main Street, Houston, USA

## ARTICLE INFO

# Keywords: Pervaporation Desalination Self-assembled sulfonated pentablock terpolymers Salt removal Permeability

## ABSTRACT

Pervaporation desalination has several advantages over competing desalination technologies, most notably an ability to select for or against volatile organic compounds and the ability to process high salinity feeds at a low transmembrane pressure. Pervaporation has not been commercialized for desalination applications because of its energy intensity. However, emerging processes such as hydraulic fracturing produce high total dissolved solids  $(>30-45~{\rm g~L}^{-1})$  byproduct streams that exceed the operational limits of traditional reverse osmosis and could be treated by pervaporation. Here, we demonstrate free-standing pervaporation membranes with excellent permeance and high salt removal based on a partially sulfonated pentablock terpolymer with the tradename Nexar<sup>TM</sup>. Pervaporation membranes were easily cast from this material with desalination performances comparable or superior to commercially available membranes. We found that the polymer degree of sulfonation and casting solvent polarity had a significant impact on the membranes' water uptake but only a modest impact on the pervaporation desalination performance. Membranes with a degree of sulfonation of 52% (2.0 meq g<sup>-1</sup> IEC) and a casting solution composed of 50 wt% n-propanol and 50 wt% toluene achieved a water flux of 3.32 kg m<sup>-2</sup>  $h^{-1}$  (permeance 135 kg m $^{-2}$   $h^{-1}$  bar $^{-1}$ ) with 99.5% salt removal in pervaporation from a 32 g  $L^{-1}$  sodium chloride feed solution at room temperature. We demonstrated that dense, non-porous Nexar™ pervaporation membrane permeance and salt separation performance were superior to commercial pervaporation membranes and equivalent to commercial membrane distillation membranes, which have much larger pores. This study demonstrates that commercially available sulfonated pentablock terpolymers are excellent membranes for pervaporation desalination because of their ease of casting and excellent performance.

## 1. Introduction

Pervaporation is a membrane separation process currently used for two distinct applications: (1) dehydration applications, such as dehydration of alcohols (e.g., ethanol) and (2) selective removal of dilute hydrophobic molecules, such as alcohol or organic solvents, from aqueous solutions [1–7]. Pervaporation is driven by a difference in vapor pressure across a membrane between the feed and permeate side, leading to selective transport of molecular species across the membrane.

This vapor pressure-driven mechanism enables multiple types of separations, such as alcohol/water separation, removal of hydrophobic or hydrophilic molecules, and retention of dissolved solids. On the latter, pervaporation is notable in its capacity to process feeds of over  $100 \, \mathrm{g \, L^{-1}}$  total dissolved solids (TDS) [8].

The capacity of pervaporation to operate at very high salinity makes it an interesting process compared to other desalination technologies; for example, applications that treat very high salinity feedwaters could potentially use pervaporation. This is a result of the fact that

<sup>\*</sup> Corresponding author. School for Engineering of Matter, Transport and Energy, Arizona State University, Tempe, AZ, 85287, USA.

<sup>\*\*</sup> Corresponding author. Department of Chemical and Biomolecular Engineering, Rice University, MS 362, 6100 Main Street, Houston, USA. E-mail addresses: mllind@asu.edu (M.L. Lind), rafaelv@rice.edu (R. Verduzco).

<sup>&</sup>lt;sup>1</sup> Equal contribution.

pervaporation has a different driving force for transport than reverse osmosis (RO), the current state of the art for desalination. Currently, RO accounts for 65% of worldwide desalination capacity and 100% of the seawater desalination technology in United States [9,10]. The driving force for RO is an applied hydraulic pressure on the feed side of the membrane that overcomes the osmotic pressure of the feed. While RO has been shown to be very energy efficient at treating solutions with a lower salinity, the increasing energy demand with increasing osmotic pressure limits most RO processes to feedwaters with a TDS of <45 g  $\rm L^{-1}$ [11,12]. Alternative low-pressure desalination processes include electrodialysis (ED) and forward osmosis (FO). ED is a mature technology that uses ion exchange membranes and an electric field gradient to facilitate the transport of ionic species, not water, for salt removal [13]. While ED is a flexible process that can handle high TDS, the capital cost of the membranes is greater than RO [14], and the specific energy consumption (kWh  $\mathrm{m}^{-3}$ ) increases with the salinity removed; therefore, above a certain salinity the energy consumption of desalination by ED would exceed that by pervaporation [15]. For FO, on the other hand, the driving force is the osmotic pressure difference between the draw and the feed solutions [16]. However, the FO process requires the use of a draw solution to create the osmotic pressure difference and the ability to recover the draw solution [17,18] – a complication that is not required with pervaporation. Specific energy consumption (SEC) provides a baseline comparison between processes. A previous study estimated SEC for pumping a pervaporation feed through a hollow fiber module as 2.0 kWh m<sup>-3</sup>, however, this did not account for the energy needed for permeate condensation [19]. MD has a high SEC estimated to be about 7.7 kWh m<sup>-3</sup> in theoretical studies [20]. Since MD and pervaporation have similar phase changes, we hypothesize that the total SEC for pervaporation is similar to MD. RO processes have variable SEC values ranging from 3.0 to 4.0 kWh  $\mathrm{m}^{-3}$  [21]. In a simulated system, FO had a theoretical minimum SEC value of 1.25–1.75 kWh  $m^{-3}$  [22]. The SEC value for ED falls ranges from 2.52 to 4.15 kWh m $^{-3}$  [23].

Pervaporation does not have the operational limitation of osmotic pressure as a driving force and thus can treat high TDS waters, such as desalination brines or produced waters, where solute concentrations can range from 60,000 to 400,000 mg  $\rm L^{-1}$  TDS [24]. The vapor pressure-driven transport in pervaporation can be compared to membrane distillation (MD), which also relies on a phase change for water transport. However, pervaporation has a number of advantages over MD. Pervaporation involves evaporation through a dense polymer membrane or microporous (pores  $\leq\!2$  nm) inorganic membrane, while MD involves evaporation though an openly macroporous (pore size  $\gg\!50$  nm) membrane. As a result, MD can have a significant problem from membrane wetting that is not encountered in pervaporation because of the difference in transport mechanism [25]. Further, unlike MD, pervaporation can select for or against volatile organic compounds.

Despite these advantages, pervaporation remains relatively unexplored for desalination. The large-scale application of pervaporation desalination has been limited by the availability of efficient, cost effective, and widely commercialized reverse osmosis (RO) which can more efficiently tackle feed waters with salinity up to the seawater range. However, regulations are evolving for the disposal of inland water treatment discharges in order to limit increases in groundwater contamination levels [26]. Simultaneously, increases in 1) hydraulic fracturing in areas such as the Marcellus, Permian, and Utica shale deposits are generating very high salinity produced wastewaters and 2) reclamation of inland brackish wastewaters (e.g., in the desert southwest of the US) is creating high salinity wastes that need to be managed [27–29]. Therefore, there is a need to develop technologies, such as pervaporation, that can reliably treat waters that have TDS level beyond the capabilities of RO.

Pervaporation membranes are typically made of dense polymeric materials, porous inorganic materials, or a composite of the two in a mixed-matrix membrane (MMM) design [30–32]. Pervaporation applications for dehydration use hydrophilic membranes with selective water

transport (e.g., cellulose acetate, poly (vinyl alcohol), or zeolites) while pervaporation applications for the removal of hydrophobic molecules from dilute aqueous solutions use hydrophobic membranes (e.g., polydimethylsiloxane, poly (1-trimethylsilyl-1-propyne), or hydrophobic zeolite imidazolate frameworks) [3-5,33]. Pervaporation membranes can either be thicker freestanding membranes (>30 µm) or thinner active layers (<2 µm) on support membranes [34–36]. For desalination applications, most pervaporation membranes reported in the literature are hydrophilic, have high salt removal (>95%), and are capable of extracting water from high salinity waters. However, limitations exist based on the type of membrane used. Zeolites and other inorganic membranes can be expensive and difficult to scale up without introducing significant defects [37–39]. Poly (vinyl alcohol) is a polymer that is soluble in water unless extensively crosslinked, and cellulose acetate has limited chemical resistance that limits the type of feeds that can be treated [8,40-43]. Other polymeric based membranes tend to have low water flux values,  $\sim 2 \text{ kg m}^{-2} \text{ hr}^{-1}$ , that must be improved prior to large scale use [19,44]. There have been several efforts to increase the water flux, with popular strategies including the use of hydrophilic polymers loaded with inorganic fillers (MMMs) or crosslinked with hydrophilic monomers [27,35,41,43,45–48]. Therefore, in analyzing the trends in the literature, it is clear that novel, inexpensive, processable, and scalable materials can help span the "valley of death" between laboratory study and commercialization.

Block polymers, by combining the properties of different polymer chemistries, can help address the different needs of pervaporation membranes for desalination, such as mechanical strength, wettability, processability, and high water flux [49-52]. Sulfonated pentablock terpolymers with the tradename Nexar<sup>TM</sup> are commercially available block polymers that have been implemented in various water treatment processes, including pervaporation dehydration, dehumidification, and electrochemical devices, but not for pervaporation desalination [50, 53-56]. These materials are attractive as membrane materials because they are easily and quickly cast from solution, have excellent mechanical properties, and exhibit excellent water uptake and transport [50,53,54, 56,57]. More interestingly, several fundamental studies have demonstrated that the morphology and performance of Nexar<sup>TM</sup> materials are strongly influenced by the polymer's degree of sulfonation [58] and polymer-solvent interactions [51,55,59]. One recent study looked at a related material, a sulfonated triblock polymer, in a pervaporation desalination process [36] and reported excellent water flux (22.87 kg  $\mathrm{m}^{-2}\,\mathrm{h}^{-1}$  at 63 °C for a 1 g  $\mathrm{L}^{-1}$  NaCl feed solution) and membrane mechanical strength. These findings suggest that Nexar<sup>TM</sup> could be a good candidate for membranes for pervaporation desalination.

The objective of this work was to study the performance of freestanding sulfonated pentablock terpolymers, or Nexar<sup>TM</sup>, as membranes for pervaporation desalination and study the relationship between polymer properties, processing conditions, membrane microstructure, and pervaporation desalination performance. To achieve these objectives, we prepared a series of membranes varying in ion-exchange capacity and casting solvent composition. We found that the pervaporation performance of the sulfonated pentablock terpolymer membranes was insensitive to changes in the membrane microstructure and water uptake. The performance was superior to commercial pervaporation membranes and on par with membrane distillation membranes. Because of the ease of membrane processing, robust mechanical properties, and excellent pervaporation desalination performance, these materials are promising candidates for use in pervaporation desalination processes and our results suggest that further optimization of the membrane processing could significantly improve performance.

# 2. Materials and methods

## 2.1. Materials

Three different polymer samples (Nexar<sup>TM</sup>) varying in degree of

sulfonation (see Table 1) were generously provided by Kraton Polymers LLC, Houston, TX, USA. These polymers were provided in solutions of approximately 11 wt % polymer dissolved in a mixture of cyclohexane/heptane. Commercial Mylar sheets (poly (ethylene terephthalate) (PET)) were generously provided by "The Griff Network" (https://www.thegriffnetwork.com/). Solvents were acquired from commercial suppliers and used as received. An unsupported poly (vinylidene fluoride) (PVDF) membrane (0.2 µm nominal pore size; Pall Corporation) was used as a MD membrane. No commercial pervaporation membranes for desalination are on the market, therefore we used commercial pervaporation membranes (PERVAP<sup>TM</sup> 4155) marketed for alcohol dehydration (ethanol and higher carbon alcohols) by DeltaMem.

## 2.2. Membrane preparation

The linear pentablock terpolymers studied are shown in Scheme 1 and contain 'A' end blocks comprised of poly (t-butyl styrene), 'B' spacer blocks of hydrogenated polyisoprene, and a 'C' midblock of partially sulfonated polystyrene in an ABCBA configuration [51,60]. Three different polymer samples were studied, varying in the degree of sulfonation of the polymer midblock: 29%, 35%, and 52% sulfonation (i.e., x in Scheme 1 equals 0.71, 0.65, and 0.48, respectively, where x represents the molar fraction of styrene relative to styrene sulfonate in the 'C' midblock), corresponding to ion exchange capacities of 1.0, 1.5, and 2.0 meg g<sup>-1</sup>, respectively. To prepare freestanding membranes, the as-received polymer solutions were first dried, then were re-dissolved in a mixture of toluene and *n*-propanol, and finally flow-coated [61] onto Mylar using a 200  $\mu$ m gap height and 2 mm s<sup>-1</sup> casting rate. The *n*-propanol content was varied over the range of 10 wt % to 50 wt %. Details of all samples studied are provided in Table 1. Tests were performed in triplicate, and average values are reported along with standard deviations.

## 2.3. Membrane characterization

## 2.3.1. Film surface morphology analysis

Surface morphology of the freestanding membranes was analyzed using Scanning Electron Microscopy (SEM, FEI Quanta 400). Membrane samples were mounted onto the SEM stub and sputter-coated with gold. Imaging was performed on both the top and cross sections of the membrane samples at 30 kV voltage.

# 2.3.2. Water uptake measurements of the membranes

Membrane water uptake was measured through gravimetric measurements [62]. Membranes were completely dried under vacuum and weighed to determine their dry weight ( $w_d$ ). The membranes were then soaked in deionized water for 24 h, removed from the water, cleaned of excess surface water by gentle wiping, then weighed to determine the wet weight ( $w_w$ ). This process was repeated four times for each sample, four replicate experiments for each sample type were performed, and average values and standard deviations were plotted. The same process was also repeated in 32 g L<sup>-1</sup> NaCl salt solutions. Using the dry and wet weight values, the % water uptake [dimensionless] is defined as [( $w_w - w_d$ )/ $w_d$ ]\*100.

**Table 1** Details for five membrane samples. IEC denotes the ion exchange capacity (meq  $g^{-1}$ ). The last column reports the weight fraction of n-propanol in the toluene/n-propanol casting solvent mixture.

Sample ID		Degree of sulfonation (mol %)	IEC (meq $g^{-1}$ )	<i>n</i> -propanol (wt %)
Sample 1		52	2.0	50
Sample 2		52	2.0	30
Sample 3		52	2.0	10
Sample 4	39		1.5	50
Sample 5	26		1.0	50

## 2.3.3. Mechanical properties of the freestanding membranes

The mechanical properties of the Nexar<sup>TM</sup> membranes and the commercial MD membranes (PALL) were measured in tensile tests using a TA Discovery HR-2. Young's Modulus, E, [MPa] of all the films was taken from the slope of the stress-strain curve. Strain [dimensionless] was determined from the crosshead displacement, and stress was calculated from the applied load normalized by the initial cross-sectional area. All films were tested at a crosshead speed of 100  $\mu m$  s $^{-1}$  at 25 °C. The dry specimens were tested with no water exposure. The wet specimens were prepared by soaking the dry specimens in water for 30 min before testing. Three specimens were tested for each sample and the mean values were reported.

# 2.3.4. Pervaporation desalination experimental setup and performance evaluation

Schematics for the pervaporation process and the bench-scale system used in this study are shown in Fig. 1. The setup consists of a recirculating feed pump, a feed reservoir, a custom-made pervaporation cell, a cold trap, and a vacuum pump. The membrane cell has a 5 cm  $\times$  5 cm active area. The cold trap consists of a glass bulb submerged in liquid nitrogen and the vacuum pump provides the necessary vapor pressure gradient for pervaporation. To evaluate the membrane performance, the membrane sample was first loaded into the pervaporation cell. To check the system for any leaks, 100 mL of DI water was circulated on the feed side of the membrane while running the permeate vacuum pump for 15 min. Then, the DI water was drained, and fresh DI water was run through the system for 1 min. Next, the DI water was completely drained out of the system and 100 mL of 32 g L<sup>-1</sup> NaCl<sub>(aq)</sub> solution was continuously circulated while the permeate side vacuum pump was turned on to allow the system to equilibrate for 30 min. To start the pervaporation desalination test, liquid nitrogen was added to the cold trap and the system was run for 30 min. The recorded permeate mass was used to calculate water flux,  $J_{water}$ , (kg m<sup>-2</sup> h<sup>-1</sup>), permeance,  $F_{water}$ , (kg m<sup>-2</sup> h<sup>-1</sup> bar<sup>-1</sup>), and permeability,  $P_{water}$ , (kg m m<sup>-2</sup> h<sup>-1</sup> bar<sup>-1</sup>) as shown in Equation (1)-3. The measured permeate conductivity values were used to calculate salt removal.

Water flux was calculated by dividing the mass of the permeate water m (kg) with the membrane area A (m<sup>2</sup>) and the experiment run time  $\Delta t$  (hr):

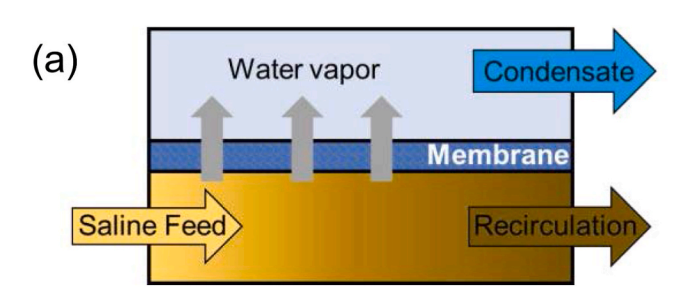
$$J_{water} = \frac{m}{A\Delta t} \tag{1}$$

Water permeance was calculated by normalizing the water flux by the differential vapor pressure,  $\Delta p^{sat}$  (bar) across the membrane:

$$F_{water} = \frac{m}{A\Delta t \Delta p^{sat}} \tag{2}$$

Water permeance allows for a more robust membrane performance comparison by accounting for variations in feed and permeate conditions, which affect the water vapor pressure. The vapor pressure on the feed side is calculated from the feed temperature and the downstream vapor pressure was assumed to be zero because of the low pressure of the vacuum pump ( $\sim 10^{-4}$  torr). The vapor pressure on the feed side is not corrected for the adjusted activity coefficient of water because of the limited difference ( $\sim$ 2%) between pure water and water with 35 g L<sup>-1</sup> of sodium chloride added, meaning it would not have had a significant impact on our results [63]. These conditions may include feed side applied pressure and temperature, permeate side vacuum, and membrane thickness. The differential vapor pressure is calculated by assuming the equilibrium vapor pressure for the liquid on the feed side and vacuum on the permeate side. The feed equilibrium vapor pressure is calculated using Antoine's equation for pure water at ambient temperature, which was measured during each individual test. The water activity coefficient is not significantly impacted by the presence of NaCl for the concentrations (32 g  $L^{-1}$ , 0.01 mol fraction NaCl) used in this study. Prior measurements of the water activity coefficient with

**Scheme 1.** Chemical structure of the Nexar<sup>TM</sup> sulfonated pentablock terpolymer.



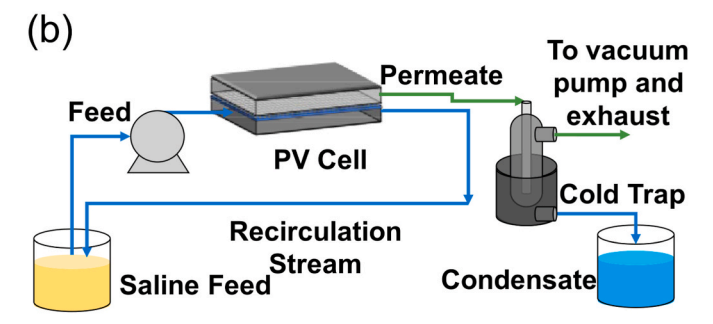


**Fig. 1.** (a) Schematic for flow streams in a pervaporation process, and (b) of the bench scale pervaporation desalination system used in this study.

dissolved NaCl predict a change of approximately 1% in the water activity coefficient for 0.01 mol fraction NaCl [64].

Permeability reflects the intrinsic water transport properties of the membrane material studied and was calculated by multiplying the water permeance by the dry membrane thickness, l (m):

$$P_{water} = \frac{ml}{A\Delta t \Delta p^{sat}} \tag{3}$$

Salt removal  $R_{salt}$  is the fraction of the feed salinity that was prevented from passing through the membrane into the permeate:

$$R_{salt} = \left(1 - \frac{c_{perm}}{c_{feed}}\right) \tag{4}$$

where,  ${}^{\prime}c_{perm}$ , and  ${}^{\prime}c_{feed}$ , are the salt concentrations (g L<sup>-1</sup>) in the permeate and feed, respectively.

# 2.3.5. Statistical analysis

We carried out statistical analyses on the resulting data, including water uptake, permeance, salt removal, and Young's modulus values for our samples. Permeance, salt removal, and Young's modulus data are all collected in triplicate for each sample type. Water uptake tests used four sample membranes for each type, with four samples taken from each membrane for a total of 16 tests per sample type. A sample set is a single membrane type (e.g., n-propanol 50%, IEC 2.0 meq g $^{-1}$ ) under a specific

testing condition (e.g., type of water for sorption or permeance testing). We used analysis of variance (ANOVA) to perform the statistical tests. ANOVA tests are null hypothesis tests that compare the means of each data set and determine if they are equal or different [65]. If they are the same, then the null hypothesis is true, and if they are different then the null hypothesis is invalid. ANOVA does not, however, identify the differences between the sample sets. Therefore, after ANOVA analysis we performed Tukey Comparison of Means with a chosen p value of <0.05, which reveals which data sets have statistically different averages and identifies those data sets [66]. These tests allow us to determine which sample sets are within the error margin of each other. On our bar graphs in this paper, statistical significance is noted by different colors (conventionally represented by different letter labels). If, for example, all bars on a graph are denoted by the color light grey (or, conventionally, the letter "a"), then they are not statistically different, and their average values are within error margins; while the bars denoted by the color dark grey (or, conventionally, the letter "b") are the same as each other and different to the light grey ("a") group. In this paper, if a bar is marked by stripes (conventionally, "ab") then it is not statistically different to either "a" or "b" groups, but "a" and "b" are different from each other. We performed all statistical analysis using OriginProTM Version 8.1 [67].

## 3. Results and discussion

## 3.1. Polymer characteristics and performance parameters

This study tested and analyzed the performance of sulfonated pentablock terpolymers for pervaporation desalination applications. All polymers had an ABCBA structure with hydrophobic poly (t-butyl styrene) 'A' blocks, hydrogenated polyisoprene 'B' blocks, and a partially sulfonated polystyrene 'C' midblock. This combination of polymer chemistries produces a robust, self-assembled membrane structure with porous domains for water transport [51,52,54]. These materials have been shown to be useful for a variety of water treatment and separation applications [50,54,56], but not for pervaporation desalination. We hypothesized that the robust mechanical properties, hydrophilicity, and tunable microstructure would enable the preparation of excellent membranes for pervaporation desalination. Three different polymer compositions varying in ion-exchange capacity were studied. The materials were dissolved in a solvent mixture of toluene and *n*-propanol, and freestanding membranes were prepared through flow-coating.

The freestanding membranes are dense, uniform films. A representative image of a 60  $\mu$ m-thick membrane sample with an ion-exchange capacity (IEC) of 2.0 meq g<sup>-1</sup> cast from 50 wt% *n*-propanol in toluene is shown in Fig. 2. The SEM micrographs show a uniform sample with no defects or pores on the surface or through cross-sectional analysis of the material. The morphology shown is representative of all membranes studied, and SEM analyses of other membrane materials are provided in the Supporting Information Fig. S1.

We measured the water uptake for all membrane materials studied. This provides useful information on the hydrophilicity of the membranes and, in general, higher water uptake correlates with higher water flux [34,41,46,68]. Fig. 3 shows that the water uptake varied widely depending on the IEC, casting solvent composition, and between DI water and NaCl solution. For all membranes studied, the water uptake was significantly higher in DI water compared with NaCl solution, and this difference increased with increasing IEC and casting solvent composition. The highest water uptake measured was 250% for the highest IEC (2.0 meq  $\rm g^{-1})$  sample studied cast from the most polar casting solvent (50 wt%  $\it n$ -propanol).

Prior work has shown that the sulfonated pentablock terpolymer membrane morphology is sensitive to both the composition of the casting solvent and the IEC of the polymer. Casting from a more polar solvent and using a polymer with higher IEC can produce a bicontinuous morphology with interconnected sulfonate domains, as was recently demonstrated [51,54], and as has been reported by the other researchers [51,53,69]. These studies have shown that the polymers are present in the form of micelles in solution, and increasing solvent polarity leads to micelle inversion with the sulfonated blocks in the corona. This inversion leads to well-connected sulfonated domains in the cast membrane which are responsible for very high water uptake as compared to the previously reported hydrophilic materials for pervaporation desalination [41,47,70,71]. Uptake of 32 g  $L^{-1}$  aq. NaCl was much lower compared with that for DI water, but uptake values as high as 100% were observed for NaCl solutions, and the uptake varied significantly with membrane IEC and casting solvent composition. For example, the NaCl solution uptake approximately doubled when the *n*-propanol content in the casting solvent increased from 10 to 50% (IEC of 2.0 meq/g) and also when the IEC was increased from 1 to 2 meq g<sup>-1</sup> (*n*-propanol content of 50%).

The mechanical properties of the membranes were studied in both the dry and wet states. Fig. 4a) and b) presents analysis of the mechanical properties of the dry and wet membranes, respectively, as a function of IEC and casting solvent composition. There is no statistically significant difference in Young's modulus between the various Nexar<sup>TM</sup> membranes under either dry or wet conditions. Furthermore, this figure indicates that the swelling led to decreased mechanical strength for all the membranes studied. The Nexar<sup>TM</sup> membranes do not have comparable mechanical strength to the commercial membranes, under either wet or dry conditions. However, unlike the commercial pervaporation membranes tested, the Nexar<sup>TM</sup> membranes are freestanding, dense membranes. Future work may include a porous support and a thin active layer. Previously, many literature studies [70,71] indicated that providing a porous support produces mechanically robust membranes and allowed reduction in the active layer thickness which can potentially decrease water transport resistance [41].

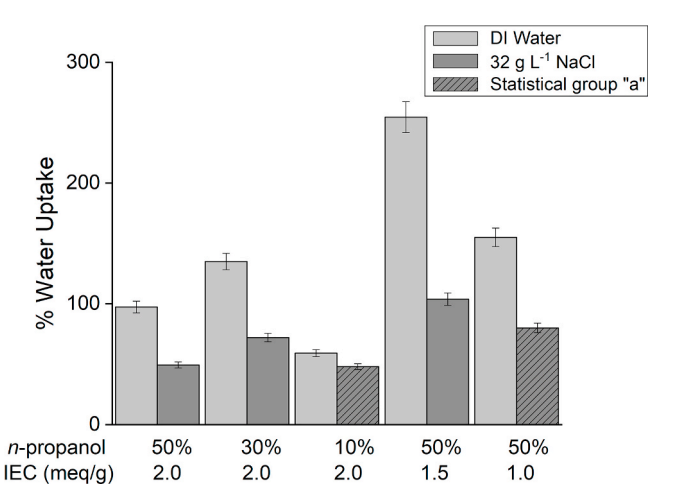


**Fig. 3.** Water uptake measurements for five types of membrane samples using DI water and 32 g L $^{-1}$  NaCl solution. Four measurements were performed for each sample and repeated four times for each sample type. A sample set is a single membrane type under a specific water uptake condition. The bars denoted with an asterisk represent sample sets (n-propanol 10%, IEC 2.0 meq/g under 32 g L $^{-1}$  conditions and n-propanol 50%, IEC 1.0 meq g $^{-1}$  under 32 g L $^{-1}$  conditions) that are statistically similarly to each other under the ANOVA and Tukey Significance test. No other samples had statistical similarity.

The performance of freestanding pentablock sulfonated polymers in pervaporation desalination was tested using the configuration shown in Fig. 1. The feedwater was 32 g  $\rm L^{-1}$  NaCl in deionized water at ambient temperatures, and vacuum was applied on the permeate side. Fig. 5 shows that for all membranes the salt removal was high (greater than 99.5%), and the average permeance values across all membranes ranged from 80 to 130 kg m $^{-2}$  h $^{-1}$  bar $^{-1}$ . We found no statistically significant difference for the permeance as a function of IEC and casting solvent polarity. The permeances of the sulfonated membranes were significantly greater than those measured for commercial pervaporation membranes and slightly greater than commercial membrane distillation membranes, despite the much larger pore structure of membrane distillation membranes.

## 3.2. Discussion on property and performance relationship

The water flux through a polymeric membrane is influenced by the membrane chemistry, hydrophilicity, morphology, and thickness [72, 73]. In our previous study, using transmission electron microscopy, we analyzed the effect of polymer ion exchange capacity and casting solvent polarities onto the membrane microstructure [54]. The results showed

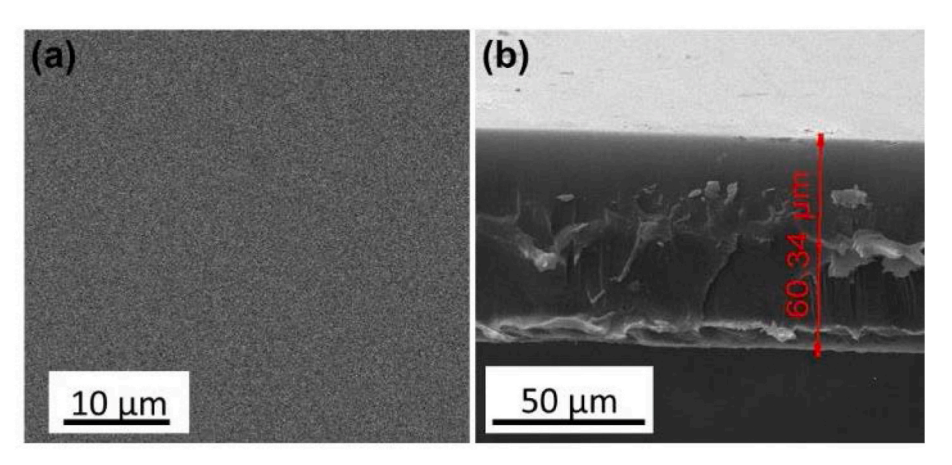
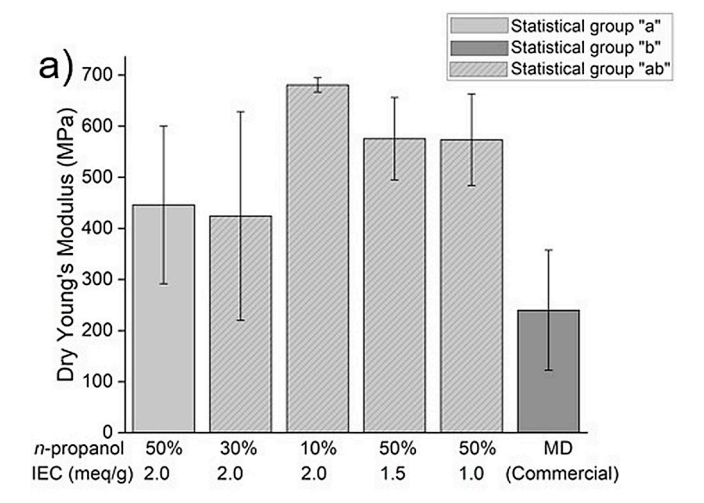
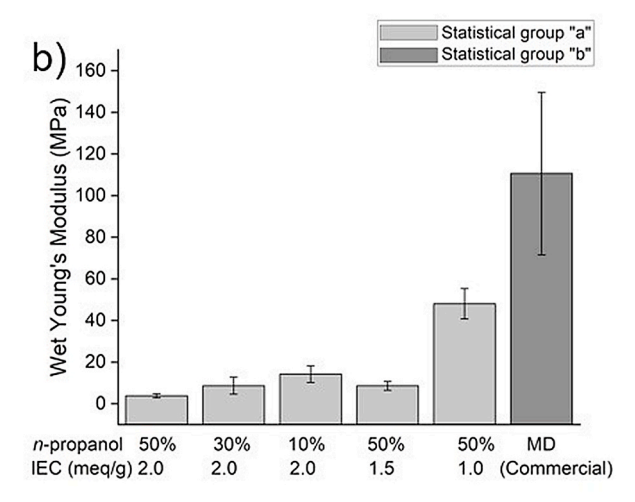


Fig. 2. (a) Top view and (b) cross-sectional SEM micrograph of freestanding membrane with an IEC of 2.0 meq g<sup>-1</sup> cast from 50 wt% *n*-propanol in toluene mixture.





**Fig. 4.** a) Young's modulus values for dry sulfonated block terpolymer membranes. b) Young's modulus values for sulfonated block terpolymer membranes tested under wet conditions. Color of bars denote statistical significance from other sample sets under an ANOVA test followed by a Tukey Significance test, with a chosen p value of <0.05. Bars with the same color are within statistical error of each other, and groups with different colors are statistically different from each other, striped bars indicate statistical similarity to both light and dark bars.

increasing both the polymer's ion-exchange capacity and casting solvent polarity leads to the inversion of the polymer micelles, subsequently leading to a membrane microstructure with well-connected sulfonated domains [54]. Here, Fig. 3 shows strong dependence of the water uptake on polymer ion exchange capacity and casting solvent polarities. However, the pervaporation desalination performance (water permeance) in Fig. 5, indicates statistically similar performance for all the samples irrespective of the polymer's ion exchange capacity, casting solvent polarities, and by extension the membrane morphology. The membrane thicknesses were similar across all samples tested, and therefore the materials had similar water permeabilities. Assuming that the solubility coefficient Kw varies linearly with the membrane water uptake, this implies that the measured permeances are roughly independent of K<sub>w</sub> and therefore water transport through the membranes is diffusion limited. This implies that reducing the thickness of the membrane could further increase membrane permeability.

# 3.3. Comparison of membranes from reported literature values

We performed a comparison of the pentablock sulfonated

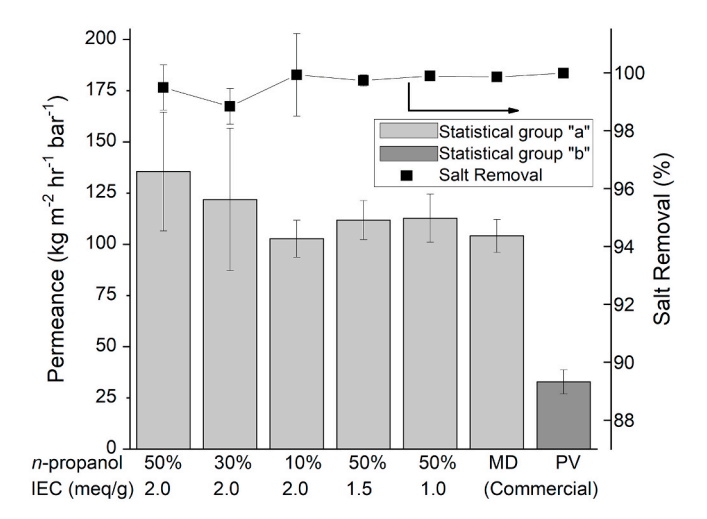


**Fig. 5.** Permeance and salt removal for varying n-propanol content in the casting solvent mixture (fixed ion-exchange capacity 2.0 meq g $^{-1}$ ). All the experiments were performed with a room temperature (approximately 21  $^{\circ}$ C) feed of 32 g L $^{-1}$  NaCl. Color of bars denote statistical significance from other sample sets under an ANOVA test followed by a Tukey Significance test, with a chosen p value of <0.05. Bars with the same color are within statistical error of each other, and groups with different colors are statistically different from each other. No statistical difference was found for salt removal (indicated by points) across all samples.

terpolymers reported here with other materials reported in the literature. Table 2 presents a comparison of water permeance and water permeability at varying feed water temperature, salinity, and membrane thickness for various pervaporation membranes. This list is not comprehensive, and the studies shown were selected because of similarities in their reported testing conditions and membrane thicknesses. Because water flux depends on the testing conditions and membrane thickness, the water permeance and permeability values were calculated for a normalized comparison. The water permeance values control for feed conditions by accounting for the vapor pressure difference in the studies reported. The water permeance values of the sulfonated pentablock terpolymer were similar [41,48,70,71,74] or lower (up to 4.25 times [47]) compared to the commercial membranes.

The permeability reflects the intrinsic water transport properties of the membrane materials, and these were calculated by multiplying the water permeance values by the membrane thickness. As shown in Table 2, the permeability of the sulfonated pentablock terpolymers was higher than most other studies listed, except for three materials: a poly (vinyl alcohol)/gluteraldehyde (GA)/laponite mixed matrix composite membrane reported by Selim et al. [47], PVA crosslinked with 4-sulfonylphthalic acid on a polysulfone support reported by Li et al. [74], and clinoptilolite phosphate reported by An et al. [75] In contrast to these studies, our materials are prepared through a simple flow-coating process of a commercially available polymer. The only material with better performance and a thicker membrane than in the present study is the Selim study, which reports a thickness of 160  $\mu m$  for a freestanding mixed matrix membrane, suggesting that the laponite in the membrane greatly enhances the transport properties.

# 4. Conclusion

We demonstrated that sulfonated pentablock terpolymers show great promise as a pervaporation desalination membrane material because of their ease of membrane synthesis, good mechanical properties, and desalination performance. We measured the water uptake, mechanical properties, and pervaporation desalination performance of these membranes and compared them to commercially available membrane distillation and pervaporation membranes. The highest performing

 Table 2

 Literature-reported membrane performance details for pervaporation desalination.

Membrane Material/Type	Feed Temp. (°C)	Conc. [NaCl] (g L <sup>-1</sup> )	Thickness (μm)	Water Flux (kg $\rm m^{-2}~hr^{-1}$ )	Permeance (kg m $^{-2}$ hr $^{-1}$ bar $^{-1}$ )	Permeability (kg m m $^{-2}$ hr $^{-1}$ bar $^{-1}$ )
Polymeric, supported membranes						
Thin film nanofibrous PVA on PAN support [70]	25	35	0.7	7.36	231	$2.0\times10^{-4}$
Crosslinked PVA on PAN support [38]***	30	35	15	8.51	205	$3.1  imes 10^{-3}$
Crosslinked PVA on PAN support [71]***	30	35	2	8	193	$4.0 \times 10^{-4}$
PVA crosslinked with 4-Sulfonylphthalic acid on polysulfone support [64]***	30	35	50	6	141	$7.1\times10^{-3}$
Inorganic, supported membranes						
Graphene oxide on PAN support [8]***	30	35	0.1	14.31	345	$3.0  imes 10^{-5}$
Mixed matrix, freestanding membranes						
PVA/GA/Laponite mixed matrix [39]***	40	30	160	38	573	$9.17 \times 10^{-2}$
PVA/maleic acid/silica hybrid mixed matrix [43] ***	22	0.2	6	6.93	380	$2.3\times10^{-3}$
Chitosan and graphene oxide mixed matrix [48]	~45	50	13	8.5	232	$3.0\times10^{-3}$
Polymer freestanding membranes						
Sulfonated Triblock Copolymer [36]***	50	10	39	8.70	135	$5.3  imes 10^{-3}$
Inorganic freestanding membranes						
Natural clinoptilolite (zeolite) [37]***	77	34	2500	0.5	1.20	$3.0  imes 10^{-3}$
Clinoptilolite phosphate [75]***	25	1.4	1.4	7	222	$3.11\times10^{-1}$
This study						
Sulfonated Pentablock Copolymer (IEC2.0, 50% np)**	20.8	32	52	3.30	135	$7.1\times10^{-3}$

**Note:** Not all papers contained information regarding the pressure differentials across the membranes, and permeance values are calculated from the best available data within the papers. Reported thickness values are the dry thickness of the membranes. Asterisks indicate whether or not any corrective factor was used to account for the salinity of the feed waters, where (\*) indicates corrected, (\*\*) indicates uncorrected, and (\*\*\*) indicates unclear.

membrane in this study had a permeance of 135.5  $\pm$  29 kg m $^{-2}$  hr $^{-1}$ bar<sup>-1</sup>, a permeability of  $7.1 \pm 1.5$  kg mm m<sup>-2</sup> hr<sup>-1</sup>, and salt removal of 99.5%. The reason for incomplete removal of non-volatile solutes in pervaporation is unclear, however, work from other prior studies suggests two potential mechanisms: First, micropores can potentially allow for the transport of salt through the membrane; second, salt may have some limited solubility in the membrane, resulting in transport through the membrane [76]. Additionally, our removal values are closely in line with reported literature values for salt removal in pervaporation desalination processes [38,41,70,77]. Interestingly, the sulfonated pentablock terpolymer polymer desalination permeance performance was superior to the commercial pervaporation membranes tested and equivalent to commercial membrane distillation membranes, which have much larger, open pores. It is important to note that there are no commercially available membranes for pervaporation desalination. Our analysis also suggested that permeabilities could be significantly increased by reducing the thickness of the membranes. Future studies of this material should investigate making thin sulfonated pentablock terpolymer on a porous support as a strategy to improve mechanical properties and increase membrane permeance.

# CRediT authorship contribution statement

Elisabeth R. Thomas: Investigation, Methodology, Formal analysis, Writing - original draft, Writing - review & editing. Amit Jain: Investigation, Methodology, Writing - original draft, Writing - review & editing. Stewart C. Mann: Methodology, Writing - review & editing. Yi Yang: Investigation, Resources, Writing - original draft. Matthew D. Green: Resources, Writing - review & editing, Funding acquisition, Project administration. W. Shane Walker: Writing - review & editing, Funding acquisition, Project administration. François Perreault: Resources, Data curation, Formal analysis, Writing - review & editing, Funding acquisition, Project administration. Mary Laura Lind: Conceptualization, Methodology, Supervision, Writing - review & editing, Funding acquisition, Project administration. Rafael Verduzco: Conceptualization, Supervision, Methodology, Writing - review & editing, Funding acquisition, Project administration.

## Declaration of competing interest

The authors declare that there is no conflict of interest.

# Acknowledgements

The authors would like to acknowledge support by the NSF Nanosystems Engineering Research Center for Nanotechnology-Enabled Water Treatment (EEC-1449500). Dr. Lind acknowledges support from NSF CAREER award #CBET-1254215. Elisabeth Thomas was partially supported by a NASA Space Technology Research Fellowship (80NSSC19K1178) and by an ASU Graduate College tuition waiver. This work has been partially supported by the Bureau of Reclamation, U.S. Department of Interior, through DWPR Agreements R16AC00125 and R19AC00088. Dr. Green and Dr. Yang's contributions were partially supported by NSF CBET award# 1836719 and ARPA-E Open award# DE-AR0001103.

# Appendix A. Supplementary data

Supplementary data to this article can be found online at https://doi.org/10.1016/j.memsci.2020.118460.

## References

- N.P. Wynn, Pervaporation, in: Kirk-Othmer Encycl. Chem. Technol., American Cancer Society, 2003, https://doi.org/10.1002/0471238961.1605182223251414. a01.
- [2] A. Yadav, M.L. Lind, X. Ma, Y.S. Lin, Nanocomposite silicalite-1/ polydimethylsiloxane membranes for pervaporation of ethanol from dilute aqueous solutions, Ind. Eng. Chem. Res. 52 (2013) 5207–5212, https://doi.org/10.1021/ ie303240f.
- [3] H. Yin, A. Khosravi, L. O'Connor, A.Q. Tagaban, L. Wilson, B. Houck, Q. Liu, M. L. Lind, Effect of ZIF-71 particle size on free-standing ZIF-71/PDMS composite membrane performances for ethanol and 1-butanol removal from water through pervaporation, Ind. Eng. Chem. Res. 56 (2017) 9167–9176, https://doi.org/10.1021/acs.iecr.7b01833.
- [4] H. Yin, C.Y. Lau, M. Rozowski, C. Howard, Y. Xu, T. Lai, M.E. Dose, R.P. Lively, M. L. Lind, Free-standing ZIF-71/PDMS nanocomposite membranes for the recovery of ethanol and 1-butanol from water through pervaporation, J. Membr. Sci. 529 (2017) 286–292, https://doi.org/10.1016/j.memsci.2017.02.006.

- [5] H. Yin, P. Cay-Durgun, T. Lai, G. Zhu, K. Engebretson, R. Setiadji, M.D. Green, M. L. Lind, Effect of ZIF-71 ligand-exchange surface modification on biofuel recovery through pervaporation, Polymer 195 (2020) 122379, https://doi.org/10.1016/j.polymer.2020.123279
- [6] R. Kreiter, D.P. Wolfs, C.W.R. Engelen, H.M. van Veen, J.F. Vente, Hightemperature pervaporation performance of ceramic-supported polyimide membranes in the dehydration of alcohols, J. Membr. Sci. 319 (2008) 126–132, https://doi.org/10.1016/j.memsci.2008.03.026.
- [7] G.M. Shi, T. Yang, T.S. Chung, Polybenzimidazole (PBI)/zeolitic imidazolate frameworks (ZIF-8) mixed matrix membranes for pervaporation dehydration of alcohols, J. Membr. Sci. 415–416 (2012) 577–586, https://doi.org/10.1016/j. memsri 2012 05 052
- [8] B. Liang, W. Zhan, G. Qi, S. Lin, Q. Nan, Y. Liu, B. Cao, K. Pan, High performance graphene oxide/polyacrylonitrile composite pervaporation membranes for desalination applications, J. Mater. Chem. A. 3 (2015) 5140–5147, https://doi. org/10.1039/C4TA06573E.
- [9] I. Ullah, M.G. Rasul, Recent developments in solar thermal desalination technologies: a review, Energies 12 (2019) 119, https://doi.org/10.3390/ en12010119
- [10] P. Rao, W.R. Morrow, A. Aghajanzadeh, P. Sheaffer, C. Dollinger, S. Brueske, J. Cresko, Energy considerations associated with increased adoption of seawater desalination in the United States, Desalination 445 (2018) 213–224, https://doi. org/10.1016/j.desal.2018.08.014.
- [11] N.P. Wynn, Pervaporation, in: Kirk-Othmer Encycl. Chem. Technol., 2003, https://doi.org/10.1002/0471238961.1605182223251414.a01.
- [12] H. Chang, T. Li, B. Liu, R.D. Vidic, M. Elimelech, J.C. Crittenden, Potential and implemented membrane-based technologies for the treatment and reuse of flowback and produced water from shale gas and oil plays: a review, Desalination 455 (2019) 34–57, https://doi.org/10.1016/j.desal.2019.01.001.
- [13] A. Campione, L. Gurreri, M. Ciofalo, G. Micale, A. Tamburini, A. Cipollina, Electrodialysis for water desalination: a critical assessment of recent developments on process fundamentals, models and applications, Desalination 434 (2018) 121–160, https://doi.org/10.1016/j.desal.2017.12.044.
- [14] S.K. Patel, M. Qin, W.S. Walker, M. Elimelech, Energy efficiency of electro-driven brackish water desalination: electrodialysis significantly outperforms membrane capacitive deionization, Environ. Sci. Technol. 54 (2020) 3663–3677, https://doi. org/10.1021/acs.est.9b07482.
- [15] W. Shane Walker, Y. Kim, D.F. Lawler, Treatment of model inland brackish groundwater reverse osmosis concentrate with electrodialysis — Part III: sensitivity to composition and hydraulic recovery, Desalination 347 (2014) 158–164, https:// doi.org/10.1016/j.desal.2014.05.034.
- [16] R.W. Field, J.J. Wu, On boundary layers and the attenuation of driving forces in forward osmosis and other membrane processes, Desalination 429 (2018) 167–174, https://doi.org/10.1016/j.desal.2017.12.001.
- [17] M. Sairam, E. Sereewatthanawut, K. Li, A. Bismarck, A.G. Livingston, Method for the preparation of cellulose acetate flat sheet composite membranes for forward osmosis—desalination using MgSO4 draw solution, Desalination 273 (2011) 299–307. https://doi.org/10.1016/j.desal.2011.01.050.
- [18] A. Shakeri, H. Salehi, M. Rastgar, Chitosan-based thin active layer membrane for forward osmosis desalination, Carbohydr. Polym. 174 (2017) 658–668, https:// doi.org/10.1016/j.carbpol.2017.06.104.
- [19] E. Korin, I. Ladizhensky, E. Korngold, Hydrophilic hollow fiber membranes for water desalination by the pervaporation method, Chem. Eng. Process. Process Intensif. 35 (1996) 451–457, https://doi.org/10.1016/S0255-2701(96)04157-8.
- [20] A. Deshmukh, C. Boo, V. Karanikola, S. Lin, A.P. Straub, T. Tong, D.M. Warsinger, M. Elimelech, Membrane distillation at the water-energy nexus: limits, opportunities, and challenges, Energy Environ. Sci. 11 (2018) 1177–1196, https://doi.org/10.1039/C8EE00291F.
- [21] G. Amy, N. Ghaffour, Z. Li, L. Francis, R.V. Linares, T. Missimer, S. Lattemann, Membrane-based seawater desalination: present and future prospects, Desalination 401 (2017) 16–21, https://doi.org/10.1016/j.desal.2016.10.002.
- [22] A. Altaee, A. Braytee, G.J. Millar, O. Naji, Energy efficiency of hollow fibre membrane module in the forward osmosis seawater desalination process, J. Membr. Sci. 587 (2019) 117165, https://doi.org/10.1016/j. memsci.2019.06.005.
- [23] P. Malek, J.M. Ortiz, H.M.A. Schulte-Herbrüggen, Decentralized desalination of brackish water using an electrodialysis system directly powered by wind energy, Desalination 377 (2016) 54–64, https://doi.org/10.1016/j.desal.2015.08.023.
- [24] D.L. Shaffer, L.H. Arias Chavez, M. Ben-Sasson, S. Romero-Vargas Castrillón, N. Y. Yip, M. Elimelech, Desalination and reuse of high-salinity shale gas produced water: drivers, technologies, and future directions, Environ. Sci. Technol. 47 (2013) 9569–9583, https://doi.org/10.1021/es401966e.
- [25] M. Khayet, T. Matsuura, Pervaporation and vacuum membrane distillation processes: modeling and experiments, AIChE J. 50 (2004) 1697–1712, https://doi. org/10.1002/aic.10161.
- [26] Environmental Protection Agency, Summary of Input on Oil and Gas Extraction Wastewater Management Practices under the Clean Water Act, 2020.
- [27] C.L. Coonrod, Y. Ben Yin, T. Hanna, A.J. Atkinson, P.J.J. Alvarez, T.N. Tekavec, M. A. Reynolds, M.S. Wong, Fit-for-purpose treatment goals for produced waters in shale oil and gas fields, Water Res. 173 (2020) 115467, https://doi.org/10.1016/j.watres.2020.115467
- [28] P. Soeth, Funding Available to Develop New Water Treatment Technologies, 2020. https://www.usbr.gov/newsroom/newsrelease/detail.cfm?RecordID=70744. (Accessed 5 June 2020).
- [29] Department of Interior, Bureau of Reclamation, Desalination and Water Purification Research Program: Research Projects for Fiscal Years 2020 and 2021,

- 2019. https://www.grants.gov/web/grants/view-opportunity.html? oppId=321236. (Accessed 5 June 2020).
- [30] P. Peng, B. Shi, Y. Lan, A review of membrane materials for ethanol recovery by pervaporation, Separ. Sci. Technol. 46 (2010) 234–246, https://doi.org/10.1080/ 01496395.2010.504681.
- [31] T.C. Bowen, R.D. Noble, J.L. Falconer, Fundamentals and applications of pervaporation through zeolite membranes, J. Membr. Sci. 245 (2004) 1–33, https://doi.org/10.1016/j.memsci.2004.06.059.
- [32] M.H.V. Mulder, J.O. Hendrickman, H. Hegeman, C.A. Smolders, Ethanol—water separation by pervaporation, J. Membr. Sci. 16 (1983) 269–284, https://doi.org/ 10.1016/S0376-7388(00)81315-0.
- [33] Y.S. Kang, E.M. Shin, B. Jung, J.-J. Kim, Composite membranes of poly(1-trimethylsilyl-1-propyne) and poly(dimethyl siloxane) and their pervaporation properties for ethanol-water mixture, J. Appl. Polym. Sci. 53 (1994) 317–323, https://doi.org/10.1002/app.1994.070530308.
- [34] W. Xie, J. Cook, H.B. Park, B.D. Freeman, C.H. Lee, J.E. McGrath, Fundamental salt and water transport properties in directly copolymerized disulfonated poly(arylene ether sulfone) random copolymers, Polymer 52 (2011) 2032–2043, https://doi. org/10.1016/j.polymer.2011.02.006.
- [35] Y.L. Xue, J. Huang, C.H. Lau, B. Cao, P. Li, Tailoring the molecular structure of crosslinked polymers for pervaporation desalination, Nat. Commun. 11 (2020) 1–9, https://doi.org/10.1038/s41467-020-15038-w.
- [36] Q. Wang, Y. Lu, N. Li, Preparation, characterization and performance of sulfonated poly(styrene-ethylene/butylene-styrene) block copolymer membranes for water desalination by pervaporation, Desalination 390 (2016) 33–46, https://doi.org/ 10.1016/j.desal.2016.04.005.
- [37] P. Swenson, B. Tanchuk, A. Gupta, W. An, S.M. Kuznicki, Pervaporative desalination of water using natural zeolite membranes, Desalination 285 (2012) 68–72, https://doi.org/10.1016/j.desal.2011.09.035.
- [38] M. Drobek, C. Yacou, J. Motuzas, A. Julbe, L. Ding, J.C. Diniz da Costa, Long term pervaporation desalination of tubular MFI zeolite membranes, J. Membr. Sci. 415–416 (2012) 816–823. https://doi.org/10.1016/j.memsci.2012.05.074.
- [39] C. Yacou, S. Smart, J.C. Diniz da Costa, Mesoporous TiO 2 based membranes for water desalination and brine processing, Separ. Purif. Technol. 147 (2015) 166–171, https://doi.org/10.1016/j.seppur.2015.04.028.
- [40] M. Naim, M. Elewa, A. El-Shafei, A. Moneer, Desalination of simulated seawater by purge-air pervaporation using an innovative fabricated membrane, Water Sci. Technol. J. Int. Assoc. Water Pollut. Res. 72 (2015) 785–793, https://doi.org/ 10.2166/wst.2015.227
- [41] B. Liang, Q. Li, B. Cao, P. Li, Water permeance, permeability and desalination properties of the sulfonic acid functionalized composite pervaporation membranes, Desalination 433 (2018) 132–140, https://doi.org/10.1016/j.desal.2018.01.028.
- [42] S.G. Chaudhri, B.H. Rajai, P.S. Singh, Preparation of ultra-thin poly(vinyl alcohol) membranes supported on polysulfone hollow fiber and their application for production of pure water from seawater, Desalination 367 (2015) 272–284, https://doi.org/10.1016/j.desal.2015.04.016.
- [43] Z. Xie, M. Hoang, T. Duong, D. Ng, B. Dao, S. Gray, Sol-gel derived poly(vinyl alcohol)/maleic acid/silica hybrid membrane for desalination by pervaporation, J. Membr. Sci. 383 (2011) 96–103, https://doi.org/10.1016/j.memsri 2011.08.036
- [44] E. Korngold, E. Korin, I. Ladizhensky, Water desalination by pervaporation with hollow fiber membranes, Desalination 107 (1996) 121–129, https://doi.org/ 10.1016/S0011-9164(96)00157-9
- [45] Y.K. Ong, G.M. Shi, N.L. Le, Y.P. Tang, J. Zuo, S.P. Nunes, T.-S. Chung, Recent membrane development for pervaporation processes, Prog. Polym. Sci. 57 (2016) 1–31, https://doi.org/10.1016/j.progpolymsci.2016.02.003.
- [46] Y. long Xue, C.H. Lau, B. Cao, P. Li, Elucidating the impact of polymer crosslinking and fixed carrier on enhanced water transport during desalination using pervaporation membranes, J. Membr. Sci. 575 (2019) 135–146, https://doi.org/ 10.1016/j.memsci.2019.01.012.
- [47] A. Selim, A.J. Toth, E. Haaz, D. Fozer, A. Szanyi, N. Hegyesi, P. Mizsey, Preparation and characterization of PVA/GA/Laponite membranes to enhance pervaporation desalination performance, Separ. Purif. Technol. 221 (2019) 201–210, https://doi. org/10.1016/j.seppur.2019.03.084.
- [48] X. Qian, N. Li, Q. Wang, S. Ji, Chitosan/graphene oxide mixed matrix membrane with enhanced water permeability for high-salinity water desalination by pervaporation, Desalination 438 (2018) 83–96, https://doi.org/10.1016/j. desal.2018.03.031.
- [49] S.P. Nunes, Block copolymer membranes for aqueous solution applications, Macromolecules 49 (2016) 2905–2916, https://doi.org/10.1021/acs. macromol.5b02579.
- [50] J. Zuo, G.M. Shi, S. Wei, T.-S. Chung, The development of novel nexar block copolymer/ultem composite membranes for C2–C4 alcohols dehydration via pervaporation, ACS Appl. Mater. Interfaces 6 (2014) 13874–13883, https://doi. org/10.1021/am503277t.
- [51] P.V. Truong, R.L. Black, J.P. Coote, B. Lee, H. Ardebili, G.E. Stein, Systematic approaches to tailor the morphologies and transport properties of solution-cast sulfonated pentablock copolymers, ACS Appl. Polym. Mater. 1 (2019) 8–17, https://doi.org/10.1021/acsapm.8b00002.
- [52] F.H. Akhtar, H. Vovushua, L.F. Villalobos, R. Shevate, M. Kumar, S.P. Nunes, U. Schwingenschlögl, K.-V. Peinemann, Highways for water molecules: interplay between nanostructure and water vapor transport in block copolymer membranes, J. Membr. Sci. 572 (2019) 641–649, https://doi.org/10.1016/j. memsci. 2018.11.050
- [53] F.H. Akhtar, H. Vovushua, L.F. Villalobos, R. Shevate, M. Kumar, S.P. Nunes, U. Schwingenschlögl, K.-V. Peinemann, Highways for water molecules: interplay

- between nanostructure and water vapor transport in block copolymer membranes, J. Membr. Sci. 572 (2019) 641–649, https://doi.org/10.1016/j.memsci.2018.11.050.
- [54] A. Jain, C. Weathers, J. Kim, M.D. Meyer, W.S. Walker, Q. Li, R. Verduzco, Self assembled, sulfonated pentablock copolymer cation exchange coatings for membrane capacitive deionization, Mol. Syst. Des. Eng. 4 (2019) 348–356, https://doi.org/10.1039/C8ME00115D.
- [55] F. Huang, T.D. Largier, W. Zheng, C.J. Cornelius, Pentablock copolymer morphology dependent transport and its impact upon film swelling, proton conductivity, hydrogen fuel cell operation, vanadium flow battery function, and electroactive actuator performance, J. Membr. Sci. 545 (2018) 1–10, https://doi. org/10.1016/j.memsci.2017.09.051.
- [56] G.M. Shi, J. Zuo, S.H. Tang, S. Wei, T.S. Chung, Layer-by-layer (LbL) polyelectrolyte membrane with Nexar<sup>TM</sup> polymer as a polyanion for pervaporation dehydration of ethanol, Separ. Purif. Technol. 140 (2015) 13–22, https://doi.org/10.1016/j.sepnur.2014.11.008.
- [57] G.M. Geise, B.D. Freeman, D.R. Paul, Characterization of a sulfonated pentablock copolymer for desalination applications, Polymer 51 (2010) 5815–5822, https://doi.org/10.1016/j.polymer.2010.09.072.
- [58] J.-H. Choi, C.L. Willis, K.I. Winey, Structure-property relationship in sulfonated pentablock copolymers, J. Membr. Sci. 394–395 (2012) 169–174, https://doi.org/ 10.1016/j.memsci.2011.12.036.
- [59] T.N. Etampawala, D. Aryal, N.C. Osti, L. He, W.T. Heller, C.L. Willis, G.S. Grest, D. Perahia, Association of a multifunctional ionic block copolymer in a selective solvent, J. Chem. Phys. 145 (2016) 184903, https://doi.org/10.1063/1.4967291.
- [60] C.L. Willis, D.L.H. Jr, S.R. Trenor, B.D. Mather, Sulfonated Block Copolymers, Method for Making Same, and Various Uses for Such Block Copolymers, 2010. US7737224 B2, http://www.google.com/patents/US7737224. (Accessed 16 September 2016).
- [61] C.M. Stafford, K.E. Roskov, T.H.E. Iii, M.J. Fasolka, Generating thickness gradients of thin polymer films via flow coating, Rev. Sci. Instrum. 77 (2006), 023908, https://doi.org/10.1063/1.2173072.
- [62] G.M. Geise, D.R. Paul, B.D. Freeman, Fundamental water and salt transport properties of polymeric materials, Prog. Polym. Sci. 39 (2014) 1–42, https://doi. org/10.1016/j.progpolymsci.2013.07.001.
- [63] O. Miyawaki, A. Saito, T. Matsuo, K. Nakamura, Activity and activity coefficient of water in aqueous solutions and their relationships with solution structure parameters, Biosci. Biotechnol. Biochem. 61 (1997) 466–469, https://doi.org/ 10.1271/bbb.61.466
- [64] O. Miyawaki, A. Saito, T. Matsuo, K. Nakamura, Activity and activity coefficient of water in aqueous solutions and their relationships with solution structure parameters, Biosci. Biotechnol. Biochem. 61 (1997) 466–469, https://doi.org/ 10.1271/bbb.61.466.

- [65] P. Goos, D. Meintrup, Statistics with JMP: Hypothesis Tests, ANOVA and Regression, John Wiley & Sons, Incorporated, New York, UNITED KINGDOM, 2016. http://ebookcentral.proquest.com/lib/asulib-ebooks/detail.action? docID=4413728. (Accessed 19 February 2020).
- [66] Tukey's test, in: G.P. Rédei (Ed.), Encycl. Genet. Genomics Proteomics Inform., Springer Netherlands, Dordrecht, 2008, https://doi.org/10.1007/978-1-4020-6754-9\_17588, pp. 2044–2044.
- [67] OriginPro 8.1 SR3, v8.1.34.90, Academic, 1991.
- [68] W. Xie, H. Ju, G.M. Geise, B.D. Freeman, J.I. Mardel, A.J. Hill, J.E. McGrath, Effect of free volume on water and salt transport properties in directly copolymerized disulfonated poly(arylene ether sulfone) random copolymers, Macromolecules 44 (2011) 4428–4438, https://doi.org/10.1021/ma102745s.
- [69] W. Zheng, C.J. Cornelius, Solvent tunable multi-block ionomer morphology and its relationship to modulus, water swelling, directionally dependent ion transport, and actuator performance, Polymer 103 (2016) 104–111, https://doi.org/10.1016/j. polymer.2016.09.055.
- [70] B. Liang, K. Pan, L. Li, E.P. Giannelis, B. Cao, High performance hydrophilic pervaporation composite membranes for water desalination, Desalination 347 (2014) 199–206, https://doi.org/10.1016/j.desal.2014.05.021.
- [71] R. Zhang, X. Xu, B. Čao, P. Li, Fabrication of high-performance PVA/PAN composite pervaporation membranes crosslinked by PMDA for wastewater desalination, Petrol. Sci. 15 (2018) 146–156, https://doi.org/10.1007/s12182-017-0204-z
- [72] Q. Wang, N. Li, B. Bolto, M. Hoang, Z. Xie, Desalination by pervaporation: a review, Desalination 387 (2016) 46–60, https://doi.org/10.1016/j. desal 2016 02 036
- [73] E. Huth, S. Muthu, L. Ruff, J.A. Brant, Feasibility assessment of pervaporation for desalinating high-salinity brines, J. Water Reuse Desalination. 4 (2014) 109–124, https://doi.org/10.2166/wrd.2014.038.
- [74] Q. Li, B. Cao, P. Li, Fabrication of high performance pervaporation desalination composite membranes by optimizing the support layer structures, Ind. Eng. Chem. Res. 57 (2018) 11178–11185, https://doi.org/10.1021/acs.iecr.8b02505.
- [75] W. An, X. Zhou, X. Liu, P.W. Chai, T. Kuznicki, S.M. Kuznicki, Natural zeolite clinoptilolite-phosphate composite Membranes for water desalination by pervaporation, J. Membr. Sci. 470 (2014) 431–438, https://doi.org/10.1016/j. memsci.2014.07.054.
- [76] E. Quiñones-Bolaños, H. Zhou, R. Soundararajan, L. Otten, Water and solute transport in pervaporation hydrophilic membranes to reclaim contaminated water for micro-irrigation, J. Membr. Sci. 252 (2005) 19–28, https://doi.org/10.1016/j. memsci.2004.10.038.
- [77] G. Liu, J. Shen, Q. Liu, G. Liu, J. Xiong, J. Yang, W. Jin, Ultrathin two-dimensional MXene membrane for pervaporation desalination, J. Membr. Sci. 548 (2018) 548–558, https://doi.org/10.1016/j.memsci.2017.11.065.